

# Corner Transfer Matrix Algorithm for Classical Renormalization Group

Tomotoshi NISHINO\* and Kouichi OKUNISHI<sup>1,\*\*</sup>

*Department of Physics, Faculty of Science, Kobe University, Rokkodai 657*

<sup>1</sup>*Department of Physics, Graduate School of Science, Osaka University, Toyonaka 560*

(Received )

We report a real-space renormalization group (RSRG) algorithm, which is formulated through Baxter's corner transfer matrix (CTM), for two-dimensional ( $d = 2$ ) classical lattice models. The new method performs the renormalization group transformation according to White's density matrix algorithm, so that variational free energies are minimized within a restricted degree of freedom  $m$ . As a consequence of the renormalization, spin variables on each corner of CTM are replaced by a  $m$ -state block spin variable. It is shown that the thermodynamic functions and critical exponents of the  $q = 2, 3$  Potts models can be precisely evaluated by use of the renormalization group method.

KEYWORDS: Density Matrix, Corner Transfer Matrix, Renormalization Group.

## §1. Introduction

The density matrix renormalization group (DMRG) established by White<sup>1,2)</sup> has greatly enhanced the applicability of the numerical real-space renormalization group (RSRG)<sup>3,4,5)</sup> to one-dimensional ( $d = 1$ ) quantum systems. After the applications to the  $S = 1$  Heisenberg spin chain,<sup>2,6,7)</sup> DMRG has been applied to a number of  $d = 1$  quantum systems, such as Heisenberg ladder,<sup>8,9,10,11)</sup> bond-alternating spin chain,<sup>12,13)</sup> strongly correlated electron system,<sup>14,15,16,25)</sup> etc. On one hand improvements upon the numerical algorithm of DMRG have been proposed in order to analyze impurity systems,<sup>18,19)</sup> random systems,<sup>20,21)</sup> Bethe lattice systems,<sup>22)</sup> correlated electron system defined in the momentum space,<sup>23)</sup> spin chains under finite temperature,<sup>24)</sup> and so on.

Recently White has analyzed the ground state wave function of  $d = 2$  quantum spin systems, using a numerically accelerated finite system DMRG algorithm.<sup>25)</sup> At first, White's acceleration technique was only applicable to the finite system DMRG algorithm. Soon after the authors extended the

---

\* e-mail: nishino@phys.kobe-u.ac.jp

\*\* e-mail: okunishi@godzilla.phys.sci.osaka-u.ac.jp

acceleration technique to infinite system DMRG algorithm.<sup>26)</sup> Further numerical acceleration in DMRG has been reported for models that have (quantum-) group symmetry.<sup>27)</sup>

The DMRG picks up relevant correlations between the local system (=block) and the rest of the system (=reservoir). Since irrelevant spin (or particle) fluctuations are projected out, the DMRG method intrinsically has a variational property. Indeed, the ground state wave function obtained by DMRG is a good variational wave function, which is written as a product of tensors.<sup>28, 29, 30)</sup> In the thermodynamic limit the tensors become position independent, where the DMRG coincides with Östlund's variational method.<sup>31, 32)</sup> Martín-Delgado, Rodríguez-Laguna and Sierra have reformulated the variational relation in DMRG using projection operators, and have proposed new RSRG algorithms.<sup>33, 34, 35)</sup>

Since  $d = 1$  quantum systems are naturally related to  $d = 2$  classical systems, it is possible to apply DMRG algorithm to the latter.<sup>36)</sup> The largest eigenvalue of the row-to-row transfer matrix is primarily important for the analysis of the  $d = 2$  classical models. The DMRG applied to a  $d = 2$  classical model evaluates the lower bound of the largest eigenvalue, using a variational state vector written in a product of tensors. It has been shown that the thermodynamic functions can be obtained precisely by DMRG in off critical regions. However, the numerical convergence in free energy becomes slow near the critical temperature, and therefore extensive computations are necessary at criticality. The reason of this slowing down is that the maximum eigenvalue of the row-to-row transfer matrix is nearly degenerate in the critical region. Such a degeneracy spoils the numerical efficiency of the Lanczos diagonalization, that is the most time consuming part in DMRG.

Baxter's method of corner transfer matrix<sup>37, 38, 39)</sup> (CTM), that was formulated in 1968 as an extension of the Kramers-Wannier approximation,<sup>40, 41)</sup> is another variational method for  $d = 2$  classical lattice systems. The method gives approximate free energy per site in the thermodynamic limit. Baxter's method seems to have no relation with DMRG, but actually both of them are deeply connected; they are both iterative renormalization group method, and have the same fixed point in the thermodynamic limit. Baxter's method can be used as a numerical method,<sup>37, 38, 39)</sup> and it runs faster than DMRG at criticality. This is because the largest eigenvalue of CTM is not degenerate even at the critical point.

In this paper we introduce the advantage of Baxter's method into the numerical algorithm of DMRG for  $d = 2$  classical system. We express the density matrix as a product of four CTMs. For the brevity, we call the improved renormalization group method 'corner transfer matrix renormalization group' (CTMRG) in the following.<sup>43)</sup> Apart from Baxter's method, the purpose of CTMRG is to obtain variational free energies of *finite size systems*, up to a certain system size.

In the next section we review the construction of CTM. In order to simplify the discussion, we consider a  $q$ -state Potts model on a decorated lattice, because it is easy to define CTM on the

lattice. In §3 we explain the variational relation in DMRG using projection operators. We then introduce CTM into the formulation of DMRG, and make up the numerical algorithm of CTMRG in §4. In §5 we apply CTMRG to  $q = 2, 3$  Potts models. It is verified via the finite size scaling analysis<sup>44, 45)</sup> that CTMRG gives correct critical exponents. Conclusions are summarized in §6.

## §2. Corner Transfer Matrix

We consider a  $q$ -state Potts model<sup>46, 47)</sup> on a decorated square lattice, whose geometry is shown in Fig.1. The white marks represent  $q$ -state spins  $\{s\}$  on vertices, and the black ones represent another set of  $q$ -state spins  $\{\sigma\}$  that are in between  $s$ -spins. We refer to the model as ‘decorated Potts model’ in the following.



Fig. 1. The  $q$ -state Potts model on a decorated lattice. The black and white marks represent  $q$ -state spin variables  $\{\sigma\}$  and  $\{s\}$ , respectively.

We consider a square shaped finite size system of linear dimension  $L$ ; the case  $L = 3$  is shown in Fig.1. The partition function is

$$Z^L = \sum_{\{\sigma\}} \sum_{\{s\}} \exp \left\{ K^* \sum_{\langle ij \rangle} \delta(\sigma_i, s_j) \right\}, \quad (2.1)$$

where  $K^*$  is the interaction parameter,  $\langle ij \rangle$  specifies the neighboring  $\sigma$ - $s$  spin pairs, and  $\delta(\sigma_i, s_j)$  is equal to unity if  $\sigma_i = s_j$  and zero otherwise. When  $q = 2$  the model coincides with the super exchange Ising model by Fisher.<sup>48)</sup> Since the decorated lattice is bipartite, we can explicitly take the configuration sum over  $\sigma$ -spins, leaving that for  $s$ -spins. The partition function after the summation

is

$$Z^L = \left( q - 2 + 2e^{K^*} \right)^M \sum_{\{s\}} \exp \left\{ K \sum_{\langle ij \rangle} \delta(s_i, s_j) \right\}, \quad (2.2)$$

where  $M = 2L(L - 1)$  is the number of  $\sigma$ -spins in the system of the linear dimension  $L$ , and  $K$  is the effective interaction parameter between  $s$ -spins;  $K$  is determined through the duality relation for the  $d = 1$  Potts model<sup>47)</sup>

$$e^K = \frac{q - 1 + e^{2K^*}}{q - 2 + 2e^{K^*}}. \quad (2.3)$$

Equation (2.2) shows that  $Z^L$  is proportional to the partition function of the Potts model on the simple square lattice.

In the same manner, we can decimate  $s$ -spins and express  $Z^L$  in eq.(2.1) as a partition function of a symmetric vertex model. The vertex weight, that represents four  $\sigma$ -spin interaction around a vertex, is expressed as

$$W_{abcd} = \sum_{s=1}^q \exp \left\{ K^* (\delta_{sa} + \delta_{sb} + \delta_{sc} + \delta_{sd}) \right\}, \quad (2.4)$$

where  $s$  represents an  $s$ -spin on the vertex, and  $a, b, c, d$  represent the  $\sigma$ -spins around  $s$ . The weight  $W_{abcd}$  is invariant under the permutations of indices, since our model is isotropic. (See eq.(2.1).) We refer to the vertex model as ‘ $q^4$ -vertex model’, since the indices  $a, b, c$ , and  $d$  run from 1 to  $q$ , and since all of the weights are nonzero.

In order to express  $Z^L$  correctly, we have to define two additional Boltzmann weights at the boundary. One is

$$P_{abc} = \sum_{s=1}^q \exp \left\{ K^* (\delta_{sa} + \delta_{sb} + \delta_{sc}) \right\} \quad (2.5)$$

that expresses the three-spin interaction at the side of the square system, and the other is

$$C_{ab} = \sum_{s=1}^q \exp \left\{ K^* (\delta_{sa} + \delta_{sb}) \right\} \quad (2.6)$$

that represents two-spin interaction at the corner. The partition function  $Z^L$  in eq.(2.1) is expressed as a tensor product of these Boltzmann weights; for example, the partition function when  $L = 3$  is

$$Z^3 = \sum_{ab\dots l} W_{kheb} P_{abc} C_{cd} P_{def} C_{fg} P_{ghi} C_{ij} P_{jkl} C_{la}, \quad (2.7)$$

where the arrangement of spin indices is shown in Fig.2.

In order to generalize the expression of  $Z^3$  in eq.(2.7) to larger systems, we introduce the half-row transfer matrix<sup>49)</sup> (HRTM) and CTM. The HRTM is the left (or the right) half of the row-to-row transfer matrix, which is a generalization of the boundary weight in eq.(2.5). The HRTM of length



Fig. 2. The symmetric  $q^4$ -vertex model that corresponds to the decorated  $q$ -state Potts model in Fig.1.

$N$  can be defined by the recursion relation

$$P_{\mathbf{abc}}^N = \sum_{d=1}^q W_{a_N d c_N b} P_{\mathbf{a'd'c'}}^{N-1}, \quad (2.8)$$

where the vector index

$$\mathbf{a} = (a_1, a_2, \dots, a_{N-1}, a_N) \quad (2.9)$$

represents a group of  $q$ -state spin indices on the half-row of length  $N$ , and  $\mathbf{a}' = (a_1, \dots, a_{N-1})$  is included in  $\mathbf{a} = (\mathbf{a}', a_N)$ ; the same for  $\mathbf{c} = (\mathbf{c}', c_N)$ . The initial value  $P_{\mathbf{abc}}^1$ , where  $\mathbf{a} = (a_1)$  and  $\mathbf{c} = (c_1)$ , is given by the boundary weight in eq.(2.5). As an example, we show the case  $N = 3$  in Fig.3. We often abbreviate the vector indices of  $P_{\mathbf{abc}}^N$  and write the HRTM as  $P_b^N$ ; in such a case we think of  $P_b^N$  as a  $q^N$ -dimensional matrix  $(P_b^N)\mathbf{ac}$ .

The CTM is a generalization of the boundary weight  $C_{ab}$  in eq.(2.6). We define CTM using the recursion relation

$$C_{\mathbf{ab}}^N = \sum_{\mathbf{c'd'}} \left( \sum_{ef} W_{e f b_N a_N} P_{\mathbf{a'e'c'}}^{N-1} P_{\mathbf{b'fd'}}^{N-1} \right) C_{\mathbf{c'd'}}^{N-1}, \quad (2.10)$$

where we have used the index rule  $\mathbf{a} = (\mathbf{a}', a_N)$  in eq.(2.9); the same for  $\mathbf{b}, \mathbf{c}$  and  $\mathbf{d}$ . The initial value  $C_{\mathbf{ab}}^1$ , where  $\mathbf{a} = (a_1)$  and  $\mathbf{b} = (b_1)$ , is given by the corner weight in eq.(2.6). Figure 4 shows the CTM when  $N = 3$ . The factor  $W P_e^{N-1} P_f^{N-1}$  inside the parenthesis in eq.(2.10) plays the role of a transfer matrix that extends the area of CTM.

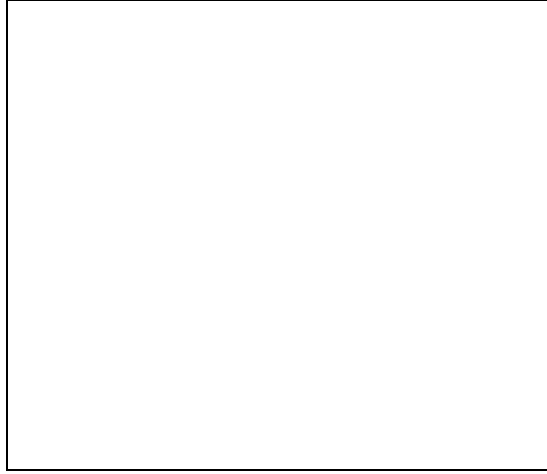


Fig. 3. The half-row transfer matrix of length 3 ( $= P^3$ ), and its components  $P^2$  and  $W$ .

It should be noted that our definition of CTM in eq.(2.10) is different from the conventional one;  $C^N$  in eq.(2.10) corresponds to a square quadrant of the whole system, while Baxter's CTM corresponds to a triangular region of a square lattice system.<sup>39)</sup> Because of this difference, two HRTMs are necessary when we increase the size of CTM. (See eq.(2.10))

We have so far chosen free boundary conditions. Since the boundary weights  $P_{abc}$  and  $C_{ab}$  in eqs.(2.5) and (2.6) determine the boundary conditions, we can impose fixed boundary conditions by modifying the definition of  $P_{abc}$  and  $C_{ab}$ . For example, if we impose  $s_i = 1$  for all  $i$ -site at the boundary, the boundary weights become

$$\begin{aligned} P_{abc} &= \exp \left\{ K^*(\delta_{1a} + \delta_{1b} + \delta_{1c}) \right\} \\ C_{ab} &= \exp \left\{ K^*(\delta_{1a} + \delta_{1b}) \right\} \end{aligned} \quad (2.11)$$

according to the fixed boundary condition.

Now we can express the partition function  $Z^L$  in terms of  $P^N$  and  $C^N$ . For even-size ( $L = 2N$ ) systems, the partition function is written as

$$Z^{2N} = \text{Tr} \left( C^N \right)^4 = \sum_{abcd} C_{ab}^N C_{bc}^N C_{cd}^N C_{da}^N. \quad (2.12)$$



Fig. 4. Corner Transfer Matrix  $C^3$ , and its components  $P^2$ ,  $C^2$ , and  $W$ . The shaded region corresponds to  $C^2$ .

For odd-size ( $L = 2N + 1$ ) cases, we generalize eq.(2.7) and express  $Z^{2N+1}$  as

$$Z^{2N+1} = \sum_{khe b} W_{khe b} \text{Tr} \left( P_k^N C^N P_h^N C^N P_e^N C^N P_b^N C^N \right) \quad (2.13)$$

where we have regarded  $P^N$  as a matrix.

In addition to the partition function, we can obtain thermal averages of the spin polarization or spin correlation functions in the same way. For example, the  $s$ -spin at the center of the odd-size ( $L = 2N + 1$ ) cluster takes the direction ‘1’ with the probability

$$\langle \delta_{1s} \rangle = \frac{\sum_{abcd} X_{abcd} \text{Tr} \left( P_a^N C^N P_b^N C^N P_c^N C^N P_d^N C^N \right)}{\sum_{abcd} W_{abcd} \text{Tr} \left( P_a^N C^N P_b^N C^N P_c^N C^N P_d^N C^N \right)}, \quad (2.14)$$

where  $X$  is a new vertex weight

$$X_{abcd} = \exp \left\{ K^* (\delta_{1a} + \delta_{1b} + \delta_{1c} + \delta_{1d}) \right\} \quad (2.15)$$

that counts the case  $s = 1$ .

The corner transfer matrix  $C^N$  is  $q^N$ -dimensional, where the dimension increases rapidly with  $N$ . The fact prevents us from exact numerical calculation of  $Z^L$  by way of eq.(2.12) and (2.13). For example when  $q = 2$ , the upper limit of  $N$  is about 13. The restriction for  $N$  is more severe for larger  $q$  cases. This is the main reason that we employ the renormalization group (RG) method.

### §3. Minimum Free Energy Principle

The background of DMRG is the minimum free energy (or the maximum partition function) principle which is represented by the density matrix. Generally speaking, a density matrix  $\rho$  in statistical mechanics is a matrix whose trace coincides with the partition function of the system. The product of four CTMs

$$\rho^{2N} = (C^N)^4 \quad (3.1)$$

is a kind of density matrix, whose trace  $\text{Tr} \rho^{2N}$  is the partition function  $Z^{2N}$  in eq.(2.12). Figure 5 shows the construction of  $\rho^{2N}$  when  $N = 3$ ; the element of the density matrix  $\rho_{\mathbf{a}\mathbf{b}}^{2N}$  represents the Boltzmann weight of the system that has a cut (or gap), where  $\mathbf{a}$  and  $\mathbf{b}$  represent the spin configurations on each side of the cut.

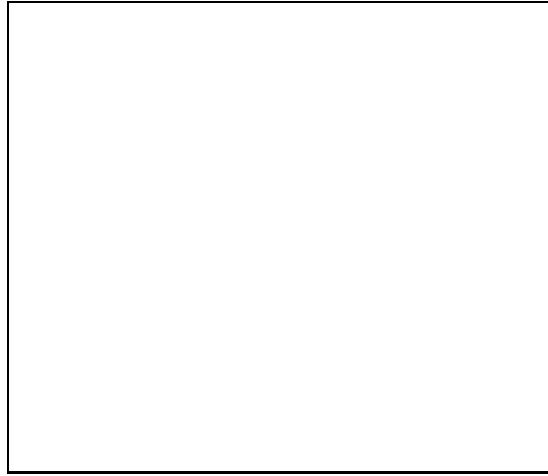


Fig. 5. Density matrix  $\rho^{2N}$  for  $N = 3$ . The shaded region represents the corner transfer matrix  $C^3$ .

Equation (3.1) shows that both  $C^N$  and  $\rho^{2N}$  have the common eigenvectors  $\mathbf{R}_i$  ( $1 \leq i \leq q^N$ ) that satisfy the eigenvalue equations

$$\begin{aligned} C^N \mathbf{R}_i &= \mathbf{R}_i \omega_i \\ \rho^{2N} \mathbf{R}_i &= \mathbf{R}_i \omega_i^4, \end{aligned} \quad (3.2)$$

where  $\omega_i$  and  $\omega_i^4$  is the  $i$ -th eigenvalue of  $C^N$  and  $\rho^{2N}$ , respectively. We write down the element of  $\mathbf{R}_i$  as  $R_{\mathbf{a}j}$  in the following. According to the symmetry of the  $q^4$ -vertex model, both  $C^N$  and  $\rho^{2N}$



are symmetric. Therefore the square matrix  $R \equiv (\mathbf{R}_1, \mathbf{R}_2, \dots)$  satisfies the orthogonal relation

$$\begin{aligned} (R^T R)_{ij} &= (\mathbf{R}_i, \mathbf{R}_j) = \delta_{ij} \\ (RR^T)_{\mathbf{ab}} &= \sum_i R_{\mathbf{a}i} R_{\mathbf{b}i} = \delta_{\mathbf{ab}}. \end{aligned} \quad (3.3)$$

We assume the decreasing order  $\omega_1^4 \geq \omega_2^4 \geq \dots$  for the eigenvalues, where all of the  $\omega_i^4$  are nonnegative; as far as our  $q^4$ -vertex model is concerned,  $\omega_i^2$  is also real and nonnegative. A trivial inequality

$$Z^{2N} \geq \sum_{\xi=1}^m \omega_{\xi}^4 \quad (3.4)$$

holds for arbitrary integer  $m$ ; the l.h.s. coincides with the r.h.s. when  $m = q^N$ , or when  $\omega_i = 0$  for all  $i > m$ . (Hereafter we use greek letters for indices that run from 1 to  $m$ .) It has been known that the dumping of  $\omega_i^4$  with respect to  $i$  is fairly rapid.<sup>2,27,39)</sup> Therefore the r.h.s. of eq.(3.4) is a good approximation for  $Z^{2N}$  for sufficiently large  $m$ . Typically  $m$  is of the order of hundreds in realistic numerical calculations.

Let us rewrite eq.(3.4) into the matrix formula

$$Z^{2N} \geq \text{Tr}(\tilde{R}\tilde{R}^T \rho^{2N}) = \sum_{\mathbf{ab}} \sum_{\xi=1}^m R_{\mathbf{b}\xi} R_{\mathbf{a}\xi} \rho_{\mathbf{ab}}^{2N} \quad (3.5)$$

where  $\tilde{R}$  is the rectangular matrix  $(\mathbf{R}_1, \mathbf{R}_2, \dots, \mathbf{R}_m)$ . The matrix product  $\tilde{R}\tilde{R}^T$  is no more an identity matrix, but is a kind of projection operator that satisfies

$$\tilde{R}\tilde{R}^T = (\tilde{R}\tilde{R}^T)^2, \quad (3.6)$$

where  $m = \text{rank}(\tilde{R}\tilde{R}^T)$  coincides with  $\text{Tr}(\tilde{R}\tilde{R}^T)$ . Let us consider a  $q^N$ -dimensional matrix  $\tilde{I}$  that satisfies  $\tilde{I} = \tilde{I}^2$  and  $\text{rank}(\tilde{I}) = m$ . One finds  $\text{Tr}(\tilde{R}\tilde{R}^T \rho^{2N}) \geq \text{Tr}(\tilde{I} \rho^{2N})$ , where the r.h.s. coincides with the l.h.s. only when  $\tilde{I} = \tilde{R}\tilde{R}^T$ . If we regard Eq.(3.5) as a variational relation for the partition function, the projection operator  $\tilde{R}\tilde{R}^T$  in eq.(3.5) gives maximum variational partition function (or minimum free energy) under the constraint  $\text{rank}(\tilde{R}\tilde{R}^T) = m$ .

We can generalize the variational relation eq.(3.5) to finite size systems with arbitrary shape. For example, let us consider an odd-size ( $L = 2N + 1$ ) square cluster, which appears in eq.(2.13) and eq.(2.15). We choose the example because it is a typical system whose density matrix is asymmetric. The density matrix is defined as

$$\rho_{\mathbf{ab}}^{2N+1} = \sum_{cdef} W_{cdef} (P_c^N C^N P_d^N C^N P_e^N C^N P_f^N C^N)_{\mathbf{ab}}, \quad (3.7)$$

where arrangements of the spin indices are shown in Fig.6. We have defined  $\rho^{2N+1}$  so that the matrix dimension coincides with that of  $\rho^{2N}$  in eq.(3.1). Since  $\rho^{2N+1}$  is asymmetric, the formulation



Fig. 6. Density matrix  $\rho^{2N+1}$  for  $N = 3$ . Unlike  $\rho^{2N}$ , the  $\rho^{2N+1}$  is not symmetric.

in eq.(3.2) and eq.(3.3) should be modified; we have to consider the left eigenvalue problem

$$\mathbf{O}_i^T \rho^{2N+1} = \lambda_i \mathbf{O}_i^T \quad (3.8)$$

independently from the right one

$$\rho^{2N+1} \mathbf{Q}_i = \mathbf{Q}_i \lambda_i, \quad (3.9)$$

where  $\lambda_i$  is the eigenvalue in the decreasing order  $\lambda_1 \geq \lambda_2 \geq \dots \geq 0$ , and  $\mathbf{O}_i$  and  $\mathbf{Q}_i$  are the left and the right eigenvector of  $\rho^{2N+1}$ , respectively. We express the vector element of  $\mathbf{O}_i$  and  $\mathbf{Q}_i$  as  $O_{\mathbf{a}i}$  and  $Q_{\mathbf{a}i}$ , respectively. This time the square matrices  $Q \equiv (\mathbf{Q}_1, \mathbf{Q}_2, \dots)$  and  $O \equiv (\mathbf{O}_1, \mathbf{O}_2, \dots)$  are not orthogonal by themselves, while they still satisfy the dual orthogonal relation

$$\left( O^T Q \right)_{ij} = (\mathbf{O}_i, \mathbf{Q}_j) = \delta_{ij}. \quad (3.10)$$

In other word,  $O^T$  is the inverse of  $Q$ . The projection operator for  $\rho^{2N+1}$ , which corresponds to  $\tilde{R}\tilde{R}^T$  in eq.(3.5), is then given by

$$\left( \tilde{Q}\tilde{O}^T \right)_{\mathbf{a}\mathbf{b}} = \sum_{\xi=1}^m Q_{\mathbf{a}\xi} O_{\mathbf{b}\xi}, \quad (3.11)$$

where  $\tilde{Q} = (\mathbf{Q}_1, \mathbf{Q}_2, \dots, \mathbf{Q}_m)$  and  $\tilde{O} = (\mathbf{O}_1, \mathbf{O}_2, \dots, \mathbf{O}_m)$  are rectangular matrices. The dual orthogonal relation eq.(3.10) ensures that the matrix  $O^T Q$  satisfies  $\left( \tilde{Q}\tilde{O}^T \right)^2 = \tilde{Q}\tilde{O}^T$  and  $\text{Tr}(\tilde{Q}\tilde{O}^T) = m$ . The inequality in partition function (eq.(3.5)) is modified to

$$Z^{2N+1} \geq \text{Tr}(\tilde{Q}\tilde{O}^T \rho^{2N+1}) \quad (3.12)$$

for the odd-size system.

We have obtained two projection operators,  $\tilde{R}\tilde{R}^T$  in eq.(3.5) and  $\tilde{Q}\tilde{O}^T$  in eq.(3.11), where they have the same matrix dimension ( $= m$ ). Since  $\tilde{R}\tilde{R}^T$  gives the maximum variational partition function when it is applied to  $\rho^{2N}$ , we obtain the relation

$$\text{Tr}(\tilde{R}\tilde{R}^T \rho^{2N}) \geq \text{Tr}(\tilde{Q}\tilde{O}^T \rho^{2N}), \quad (3.13)$$

where the r.h.s. approaches to the l.h.s. with increasing  $m$ . Conversely, we have

$$\text{Tr}(\tilde{Q}\tilde{O}^T \rho^{2N+1}) \geq \text{Tr}(\tilde{R}\tilde{R}^T \rho^{2N+1}). \quad (3.14)$$

Let us compare the even-size system in Fig.5 with the odd-size one in Fig.6. Both of them have the same cut (or gap) of length  $N = 3$ , but their system sizes are different. The inequalities eq.(3.13) and eq.(3.14) show that each system has its own optimal projection operator, that is not the optimal one of other systems. The ratio

$$\text{Tr}(\tilde{R}\tilde{R}^T \rho^{2N+1}) / \text{Tr}(\tilde{Q}\tilde{O}^T \rho^{2N+1}) \quad (3.15)$$

depends on how the density matrix catches the boundary effect. If the system is off-critical (or massive), the boundary effect is expected to disappear in the thermodynamic limit  $N \rightarrow \infty$ , and therefore the ratio eq.(3.15) approaches to unity with increasing  $N$ . Even for a system at criticality, it is numerically observed that the ratio approaches to unity with increasing  $N$ .

#### §4. Renormalization group algorithm

The projection operator  $\tilde{R}\tilde{R}^T$  in eq.(3.5) restricts the degree of freedom of  $\rho^{2N}$  down to  $m$ . Therefore the operation of the matrix  $\tilde{R}$  on  $\rho^{2N}$  can be regarded as a RG transformation. In this sense the  $m$ -dimensional diagonal matrix

$$\tilde{\rho}^{2N} = \tilde{R}^T \rho^{2N} \tilde{R} = \text{diag}(\omega_1^4, \omega_2^4, \dots, \omega_m^4). \quad (4.1)$$

is the renormalized density matrix, that satisfies the variational relation

$$Z^{2N} \geq \text{Tr} \tilde{\rho}^{2N} = \text{Tr}(\tilde{R}\tilde{R}^T \rho^{2N}). \quad (4.2)$$

Since  $\rho^{2N}$  is written as a product of four CTMs, the RG transformation in eq.(4.2) can be naturally extended to CTM:

$$\tilde{C}^N = \tilde{R}^T C^N \tilde{R} = \text{diag}(\omega_1, \omega_2, \dots, \omega_m). \quad (4.3)$$

There are several ways to define the RG transformation for HRTM. A way is to use the variational relation for  $Z^{2N+1}$  in eq.(3.12). Since  $\rho^{2N+1}$  contains  $P_a^N$  as shown in eq.(3.7), the rectangular matrix  $\tilde{O}$  in eq.(3.12) transforms  $P_a^N$  as  $\tilde{O}^T P_a^N \tilde{O}$ . However, we don't follow this way, because the renormalized HRTM thus defined is not consistent with the renormalized CTM in eq.(4.2). In

order to avoid the problem, we define the RG transformation for HRTM using another variational relation

$$Z^{2N+1} \geq \text{Tr}(\tilde{R}\tilde{R}^T\rho^{2N+1}), \quad (4.4)$$

which is derived from eq.(3.12) and eq.(3.14). This time  $\tilde{R}$  touches  $P_a^N$ , which exists inside  $\rho^{2N+1}$ . (See Eq.(3.7)) From eq.(4.4), we can define the renormalized HRTM as

$$\tilde{P}_a^N = \tilde{R}^T P_a^N \tilde{R}, \quad (4.5)$$

where the  $(\xi\eta)$  element of  $\tilde{P}_a^N$  is  $\tilde{P}_{\xi a \eta}^N$ .



Fig. 7. Extension of the renormalized CTM. Note that  $\tilde{C}^N$  is a diagonal matrix.

Now we explain the detail of our RG algorithm, that extends the system size recursively using a mapping from  $\tilde{C}^N$  and  $\tilde{P}_a^N$  to  $\tilde{C}^{N+1}$  and  $\tilde{P}_a^{N+1}$ , respectively. Remember that  $C^N$  is defined recursively in eq.(2.8). It is possible to generalize the recursion relation to the renormalized CTM in eq.(4.3)

$$\bar{C}_{(\alpha,a)(\beta,b)}^{N+1} = \sum_{ef\delta} W_{efba} \tilde{P}_{\alpha e \delta}^N \tilde{P}_{\beta f \delta}^N \tilde{C}_{\delta\delta}^N, \quad (4.6)$$

where  $\bar{C}_{(\alpha,a)(\beta,b)}^{N+1}$  is an extended CTM of linear size  $N+1$ , and the pairs of indices  $(\alpha, a)$  and  $(\beta, b)$  represent the row and the column indices of the  $qm$ -dimensional matrix  $\bar{C}^{N+1}$ . (Fig.7) We have used the fact that  $\tilde{C}^N$  is diagonal:  $\tilde{C}_{\alpha\beta}^N = \delta_{\alpha\beta}\omega_\alpha$ . The matrix  $\bar{C}^{N+1}$  is ‘partially diagonalized’ in the sense that it contains  $m$ -state block-spin indices  $\alpha$  and  $\beta$ . We then perform the renormalization

group transformation on  $\bar{C}^{N+1}$  and decrease its matrix dimension ( $= qm$ ) down to  $m$ . For this purpose we create the density matrix for the extended system

$$\bar{\rho}^{2(N+1)} = \left(\bar{C}^{N+1}\right)^4, \quad (4.7)$$

and solve the eigenvalue problem

$$\bar{\rho}^{2(N+1)} \bar{\mathbf{R}}_i = \bar{\mathbf{R}}_i \lambda_i \quad (4.8)$$

in order to create a new RG transformation matrix  $\bar{R} = (\bar{\mathbf{R}}_1, \bar{\mathbf{R}}_2, \dots, \bar{\mathbf{R}}_m)$ , where the eigenvalues  $\lambda_i$  are in the decreasing order. As we have done in eq.(4.3), we perform RG transformation for  $\bar{C}^{N+1}$  as

$$\tilde{C}^{N+1} = \bar{R}^T \bar{C}^{N+1} \bar{R}, \quad (4.9)$$

to obtain the new renormalized CTM  $\tilde{C}^{N+1}$ , which is an  $m$ -dimensional diagonal matrix. We also perform the RG transformation for HRTM at the same time. First we increase the length of HRTM using the relation

$$\bar{P}_{(\alpha,a)b(\gamma,c)}^{N+1} = \sum_{d=1}^q W_{adcb} \tilde{P}_{\alpha d \gamma}^N \quad (4.10)$$

which is a generalization of eq.(2.8), and then renormalize  $\bar{P}_b^{N+1}$  by applying  $\bar{R}$  to  $\bar{P}_b^{N+1}$ :

$$\tilde{P}_a^{N+1} = \bar{R}^T \bar{P}_a^{N+1} \bar{R}. \quad (4.11)$$

In this way, we have obtained  $\tilde{C}^{N+1}$  and  $\tilde{P}^{N+1}$  from  $\tilde{C}^N$  and  $\tilde{P}^N$  through eqs.(4.6)-(4.11). This is a cycle in CTMRG. Since the matrix dimension of  $\tilde{C}^N$  in eq.(4.6) is equal to (or less than)  $qm$ , we can repeat the RG process up to arbitrary  $N$ . Compare to Baxter's method<sup>37,38,39</sup>, the process of the renormalization group transformation (eq.(4.9)) is the same, but the way to extend CTM (eq.(4.6)) is different; the chief difference is that the renormalized HRTM appears explicitly in CTMRG, while it is absent in Baxter's method.

The maximum matrix element in  $\tilde{C}^N$  and  $\tilde{P}^N$  grows exponentially with respect to  $N$ , since free energy is extensive. Therefore we should take an appropriate normalization for both  $\tilde{C}^N$  and  $\tilde{P}^N$  during the iteration. The simplest way is just to divide these matrices by their largest element, and store the normalization factor.

Every after the iteration, the variational (or the approximate) partition function is obtained from the relations  $\tilde{Z}^{2N} = \text{Tr}(\tilde{C}^N)^4$ , or

$$\tilde{Z}^{2N+1} = \sum_{kheb} W_{kheb} \text{Tr}(\tilde{P}_k^N \tilde{C}^N \tilde{P}_h^N \tilde{C}^N \tilde{P}_e^N \tilde{C}^N \tilde{P}_b^N \tilde{C}^N). \quad (4.12)$$

Thermodynamic functions can be calculated from the numerical derivative of the variational free energy  $\tilde{F} = -k_B T \ln \tilde{Z}^{2N}$  with respect to the temperature. Spin polarization and correlation functions can be expressed as a product of renormalized CTM and HRTM. For example, spin

polarization at the center of the odd-size system is calculated as

$$\langle \delta_{1s} \rangle = \frac{\sum_{abcd} X_{abcd} \text{Tr} \left( \tilde{P}_a^N \tilde{C}^N \tilde{P}_b^N \tilde{C}^N \tilde{P}_c^N \tilde{C}^N \tilde{P}_d^N \tilde{C}^N \right)}{\sum_{abcd} W_{abcd} \text{Tr} \left( \tilde{P}_a^N \tilde{C}^N \tilde{P}_b^N \tilde{C}^N \tilde{P}_c^N \tilde{C}^N \tilde{P}_d^N \tilde{C}^N \right)}, \quad (4.13)$$

which is the renormalized expression for eq.(2.14). As shown in eq.(4.12) and eq.(4.13), the renormalized system of size  $L = 2N + 1$  has original  $q$ -state spin variables at the center. Therefore local quantities at the center are most easily obtained.

The algorithm of CTMRG is closely related to the infinite system algorithm in DMRG.<sup>1)</sup> Okunishi have investigated their common thermodynamic limit.<sup>42)</sup> The major difference between DMRG and CTMRG is that the DMRG create density matrix using an eigenvector of the row-to-row transfer matrix, while in CTMRG the density matrix is expressed as a product of four CTMs. In other word, DMRG treats an infinitely long  $d = 2$  system of width  $L$ , while CTMRG treats a square shaped finite size system of size  $L$ .

We have treated the symmetric  $q^4$ -vertex model as a reference system. It is straightforward to apply the CTMRG to other systems, such as the  $J_1$ - $J_2$  Ising model,<sup>50, 51, 52)</sup> the IRF model, and triangular systems. Speaking more generally, CTMRG is applicable to periodic  $d = 2$  classical lattice systems that have short-range interactions and discrete spin (or site) variables. Since the CTM of these models are not always symmetric, care must be taken for the diagonalization of the density matrix; we don't explain the detail here because it is rather lengthy.<sup>53)</sup>

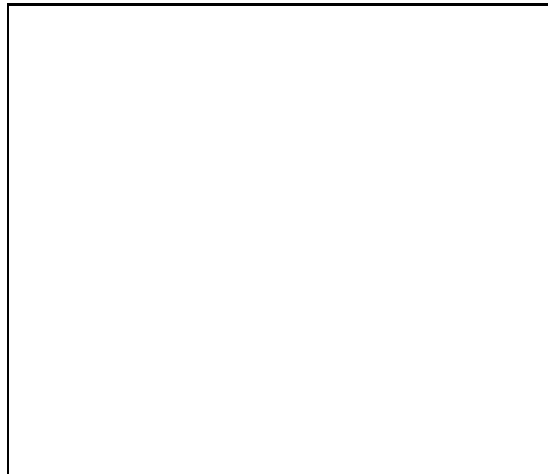


Fig. 8. A cut of length 3 on the  $d = 2$  lattice. The cut touches the shaded 3 by 3 square block.

In closing this section, we comment on the relation between the conventional block RG<sup>3)</sup> and CTMRG. Let us consider an infinitely large square lattice that has a cut of length 3. (Fig.9) As we have defined the density matrix for systems in Figs.5-6, we can define  $q^3$ -dimensional density matrix that corresponds to the cut (or gap) in Fig.9. The density matrix naturally leads a RG transformation  $\tilde{R}$  as we have mentioned in eq.(4.2), where  $\tilde{R}$  transforms a set of 3 spins into an  $m$ -state block spin variable. By applying the block spin transformation for every side of the shaded square, we can map the 3 by 3 cluster into a  $m^4$ -vertex. The CTMRG can be interpreted as a kind of block RG, where the block size is equal to a quadrant of the whole system.

## §5. Numerical Results

The decorated Potts model, which we have treated as a  $q^4$ -vertex model, has one-to-one correspondence to the Potts model on the simple square lattice; see eqs.(2.1)-(2.3). Hereafter we refer to the latter simply as ‘Potts model’. Using the correspondence, we perform numerical calculations for  $q^4$ -vertex model and observe the scaling behavior of the  $q = 2, 3$  Potts model at criticality

$$K_c = \ln(\sqrt{q} + 1). \quad (5.1)$$

We examine the calculated data using finite size scaling,<sup>44, 45)</sup> and compare the evaluated critical exponents  $\eta$  and  $\nu$  with exact ones.

The order parameter of the  $q$ -state Potts model is defined as<sup>47)</sup>

$$M \equiv \frac{q\langle\delta_{1s}\rangle - 1}{q - 1}. \quad (5.2)$$

At the center of square cluster, it is expected that the local order parameter  $M$  obeys the scaling formula

$$M \sim L^{-(d-2+\eta)/2} \quad (5.3)$$

at criticality, where  $d$  is the spatial dimension ( $= 2$ ), and  $L$  is the linear dimension of the system. We impose fixed boundary conditions in eq.(2.11), because otherwise  $\langle\delta_{1s}\rangle$  is always zero. We evaluate  $\langle\delta_{1s}\rangle$  using eq.(4.13).

Figure 9 shows the system size dependence of the order parameter  $M$  in eq.(5.2) of the  $q = 2$  Potts model, i.e., the Ising model. We plot representative data when  $m = 4$  and  $m = 200$ . The parameter  $M$  is almost proportional to  $L^{-1/8}$ , which is consistent with the finite size scaling behavior in eq.(5.2) with  $\eta = 1/4$ . In fact, the least-square fitting to the calculated data in the range  $10 \leq L \leq 1000$  gives  $\eta = 0.2504$ . We also perform the same scaling analysis for the  $q = 3$  Potts model. The obtained  $\eta$  when  $m = 200$  is summarized in Table I. The calculated exponents are in accordance with the exact results.<sup>47, 54)</sup>



Fig. 9. Log-scale plot of the order parameter  $M$  in eq.(5.1) of the  $q = 2$  Potts model.

Table I. Critical exponents  $\eta$  of the  $q = 2, 3$  Potts Models. Least-square fittings are done in two regions,  $10 \leq L \leq 1000$  and  $100 \leq L \leq 1000$ .

q	Exact	$L = 10 \sim 1000$	$L = 100 \sim 1000$
2	$1/4 = 0.25$	0.2504	0.2501
3	$4/15 = 0.2\dot{6}$	0.2652	0.2654

We calculate another critical exponent  $\nu$  using the finite size scaling behavior of the local energy

$$E - E_c \sim L^{1/\nu-d} \quad (5.4)$$

at criticality, where  $E$  is the nearest neighbor spin correlation function

$$E = \langle \delta(s_i, s_{i+1}) \rangle, \quad (5.5)$$

and  $E_c$  is the local energy per site in the thermodynamic limit  $L \rightarrow \infty$ . The value of  $E_c$  is equal to<sup>47, 39)</sup>

$$E_c = \frac{1}{2} + \frac{1}{2\sqrt{q}}, \quad (5.6)$$



where the value comes from the duality relation.<sup>47)</sup> Table II shows the calculated exponents  $\nu$  for  $q = 2, 3$  Potts models when  $m = 200$ . The calculated exponents agree with the exact ones.<sup>47, 54)</sup>

One of the recent Monte Carlo (MC) simulation up to  $N = 512$  by Swendsen-Wang algorithm<sup>55)</sup> gives the exponent  $\nu = 0.835(2)$  for the case  $q = 3$ .<sup>56)</sup> Therefore, the numerical precision of the CTMRG method is comparable to that of the recent MC simulation. The superiority of the CTMRG is that the computation time is proportional to  $N$ , while it is proportional to  $N^2$  in MC simulation. In addition, it should be noted that MC simulation requires several independent runs in order to collect scaling data; in CTMRG one can obtain the scaling data at once by single run.

Table II. Critical exponents  $\nu$  of the  $q = 2, 3$  Potts Models.

q	Exact	$L = 10 \sim 1000$	$L = 100 \sim 1000$
2	1	1.0017	1.0006
3	$5/6 = 0.8\dot{3}$	0.8323	0.8321

We finally compare the numerical convergence in CTMRG to that in Baxter's variational method.<sup>37, 38, 39)</sup> Figure 10 shows the number of iterations that are necessary for obtaining site energy of  $q = 2$  potts model; we stop the iteration when the second largest eigenvalue of the renormalized CTM converges down to the precision  $10^{-8}$  under the condition  $m = 20$ . The thick line shows the iteration number by CTMRG, and the thin line shows that by Baxter's variational method. Throughout the whole temperature region, CTMRG exhibits better numerical convergence than Baxter's method. In particular, at the temperature shown by the cross marks, the calculation by Baxter's method is 'trapped' at a quasi stable point, and therefore the obtained results are not correct; such an instability does not occur in CTMRG.

## §6. Conclusion

We have explained the minimum free energy principle, which is the common back ground in both DMRG and Baxter's CTM method. From the variational view point, we introduce the concept of DMRG into Baxter's method, and obtain a new RG method for  $d = 2$  classical lattice models. Apart from the original DMRG, the numerical algorithm of our method (CTMRG) is stable even at the critical point.

In order to check the efficiency of CTMRG, trial calculations are performed for  $q = 2, 3$  Potts

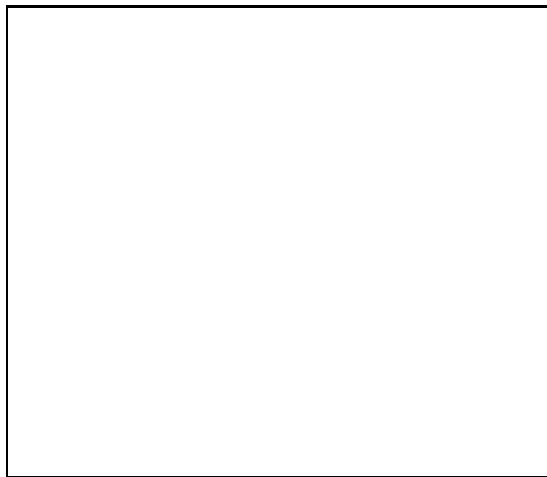


Fig. 10. Number of numerical iterations that are necessary for obtaining site energy. The thick line shows the number by CTMRG, and the thin line shows that by Baxter's variational method. At the point shown by the marks, the free energy did not obtained correctly by Baxter's method.

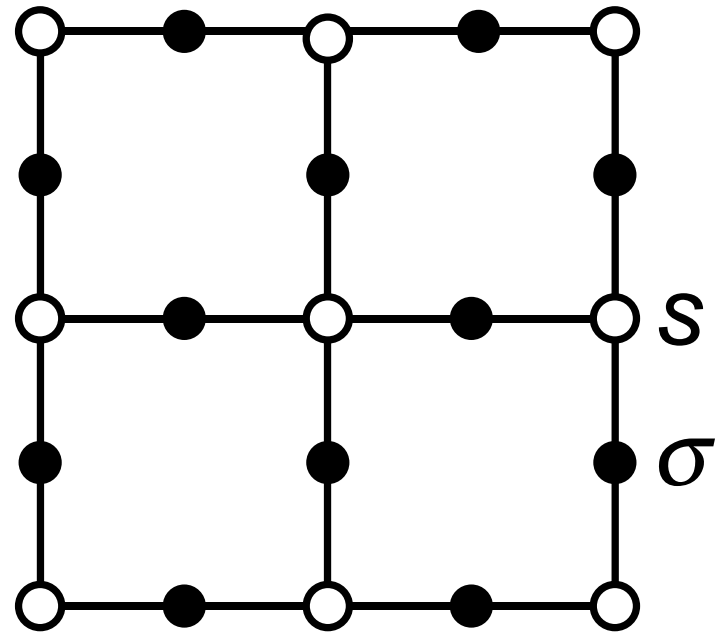
models at criticality. Calculated data are analyzed using the finite size scaling method, and it is confirmed that critical exponents of these models are correctly evaluated by CTMRG.

The authors would like to express their sincere thanks to Y. Akutsu and M. Kikuchi for valuable discussions. T. N. thank to G. Sierra, M. A. Martín-Delgado, and S. R. White for helpful discussions about DMRG. K. O. is supported by JSPS Research Fellowships for Young Scientists. The present work is partially supported by a Grant-in-Aid from Ministry of Education, Science and Culture of Japan. Most of the numerical calculations were done by NEC SX-3/14R in computer center of Osaka University.

- 
- [1] S. R. White: Phys. Rev. Lett. 69 (1992) 2863.
  - [2] S. R. White: Phys. Rev. B48 (1993) 10345.
  - [3] L. P. Kadanoff: Physics 2 (1965) 263.
  - [4] K. G. Wilson and J. Kogut: Phys. Rep. 12C (1974) 75.
  - [5] T. W. Burkhardt and J. M. J. van Leeuwen: *Real-Space Renormalization*, Topics in Current Physics vol.**30**, (Springer, Berlin, 1982), and references there in.
  - [6] S. R. White and D. A. Huse: Phys. Rev. **B48** (1993) 3844.
  - [7] E. S. Sorensen and I. Affleck: Phys. Rev. **B49** (1994) 15771.
  - [8] K. Hida: J. Phys. Soc. Jpn. **64** (1995) 4896.
  - [9] S. R. White: Phys. Rev. **B53** (1996) 52.
  - [10] U. Schollwöck and David Y. K. Ko: Phys. Rev. **B53** (1996) 240.

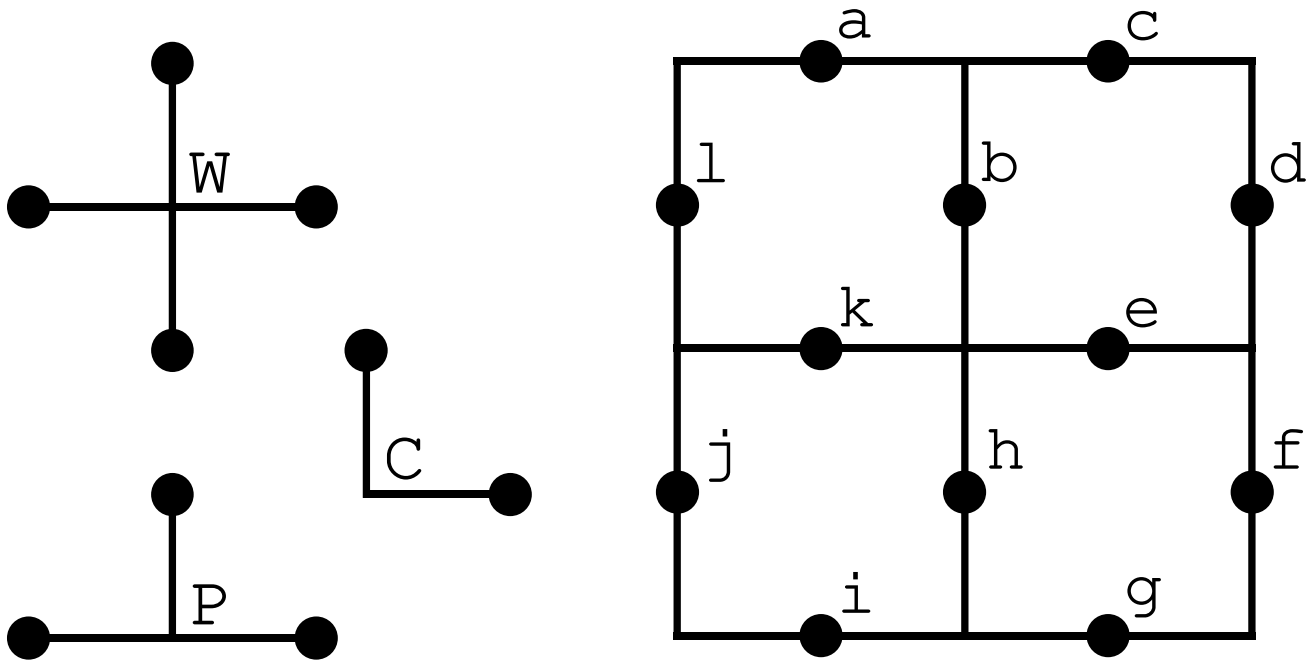
- [11] S. R. White and I. Affleck: Phys. Rev. **B54** (1996) 9862.
- [12] Y. Kato and A. Tanaka: J. Phys. Soc. Jpn. **63** (1994) 1277.
- [13] M. Yajima and M. Takahashi: J. Phys. Soc. Jpn. **65** (1996) 39.
- [14] C. C. Yu and S. R. White: Phys. Rev. Lett. **71** (1993) 3866.
- [15] R. M. Noack, S. R. White and D. J. Scalapino: Phys. Rev. Lett **73** (1994) 882.
- [16] N. Shibata, T. Nishino, K. Ueda and C. Ishii: Phys. Rev. **B53** (1996) R8828.
- [17] S. R. White: preprint, cond-mat/9605143.
- [18] E. S. Sorensen and I. Affleck: Phys. Rev. **B51** (1995) 16115.
- [19] X. Wang and S. Mallwitz: Phys. Rev. **B53** (1996) R492.
- [20] K. Hida: J. Phys. Soc. Jpn. **65** (1996) 895.
- [21] K. Hida: preprint, cond-mat/9612232.
- [22] H. Otsuka: Phys. Rev. **53** (1996) 14004.
- [23] T. Xiang: Phys. Rev. **53** (1996) R10445.
- [24] R. J. Bursill, T. Xiang, and G. A. Gehring: J. Phys. C **8** (1996) L1-L8.
- [25] S. R. White: preprint cond-mat/9604129.
- [26] T. Nishino and K. Okunishi: J. Phys. Soc. Jpn. **64** (1995) 4084.
- [27] G. Sierra and T. Nishino: will appear in Nucl. Phys. B, preprint cond-mat/9610221.
- [28] A. Klümper, A. Schadschneider and J. Zittarz: Z. Phys. B87 (1992) 281.
- [29] A. Klümper, A. Schadschneider and J. Zittarz: Europhys. Lett. 24 (1993) 293.
- [30] A. Schadschneider and J. Zittarz: Ann. Physik 4 (1995) 157.
- [31] S. Östlund and S. Rommer: Phys. Rev. Lett **75** (1995) 3537.
- [32] S. Rommer and S. Östlund: preprint, cond-mat/9606213.
- [33] M. A. Martín-Delgado and G. Sierra: Int. J. Mod. Phys **A11** (1996) 3145.
- [34] M. A. Martín-Delgado, J. Rodriguez-Laguna and G. Sierra: Nuc. Phys. B473 (1996) 685.
- [35] M. A. Martín-Delgado and G. Sierra: UCM/CSIC-96-01 preprint July 1996.
- [36] T. Nishino, J. Phys. Soc. Jpn. 64, No.10 (1995) 3598.
- [37] R. J. Baxter: J. Math. Phys. 9 (1968) 650 .
- [38] R. J. Baxter: J. Stat. Phys. 19 (1978) 461.
- [39] R. J. Baxter: *Exactly Solved Models in Statistical Mechanics* (Academic Press, London, 1982) p.363.
- [40] H. A. Kramers and G. H. Wannier, Phys. Rev. 60 (1941) 263.
- [41] R. Kikuchi, Phys. Rev. 81 (1951) 988.
- [42] K. Okunishi: Thesis (in Japanese), Osaka University (1996).
- [43] T. Nishino and K. Okunishi: J. Phys. Soc. Jpn. **65** (1996) 891.
- [44] M. E. Fisher, in *Proc. Int. School of Physics 'Enrico Fermi'*, edited by M.S. Green, (Academic Press, New York, 1971), Vol. 51, p. 1.
- [45] M. N. Barber: in *Phase Transitions and Critical Phenomena*, edited by C. Domb and J.L. Lebowitz, (Academic Press, New York, 1983), Vol. 8, p. 146. and references therein.
- [46] R. B. Potts: Proc. Camb. Phil. Soc.**48** 106.
- [47] F. Y. Wu: Rev. Mod. Phys. **54** (1982) 235, and references there in.
- [48] M. E. Fisher: Proc. Roy. Soc. **A254** (1960) 502.
- [49] The half-row transfer matrix is sometimes called as 'vertex operator'.
- [50] J. Kanamori: Prog. Theor. Phys. **35** (1966) 17.
- [51] K. Tanaka, T. Horiguchi, and T. Morita: Phys. Lett. **A165** (1992) 266.

- [52] K. Tanaka, T. Horiguchi, and T. Morita: Prog. Theor. Phys. **115** Suppl. (1994) 221.
- [53] The matrix operations for such asymmetric CTMs are explained by Baxter in his textbook<sup>39)</sup> p. 380.
- [54] D. Friedan, Z. Qiu, and S. Shenker: Phys. Rev. Lett. **52** (1984) 1575.
- [55] R. H. Swendsen and J. -S. Wang: Phys. Rev. Lett. **58** (1987) 86.
- [56] J. Salas and A. D. Sokal: preprint, hep-lat/9605018 v2 19 Feb 97.



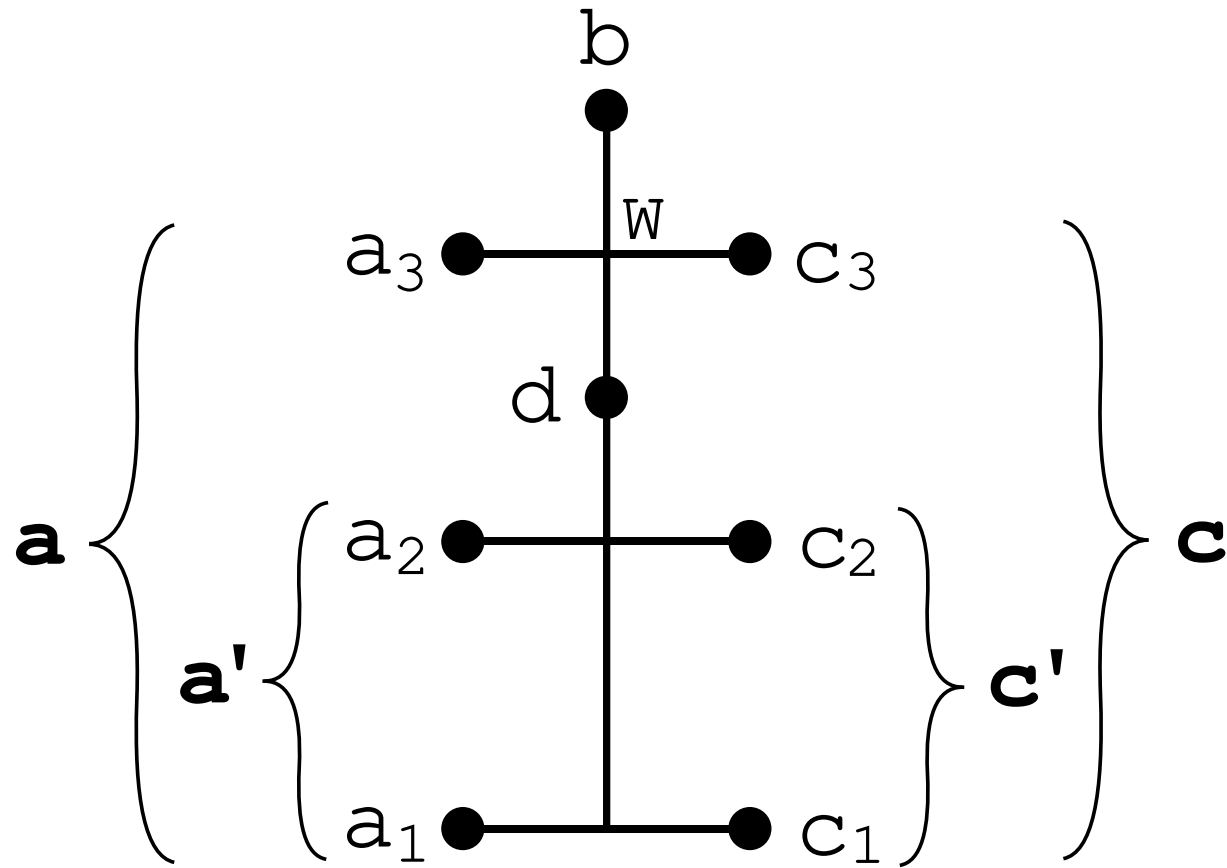
- Fig.1 -

**T. Nishino**  
**K. Okunishi**



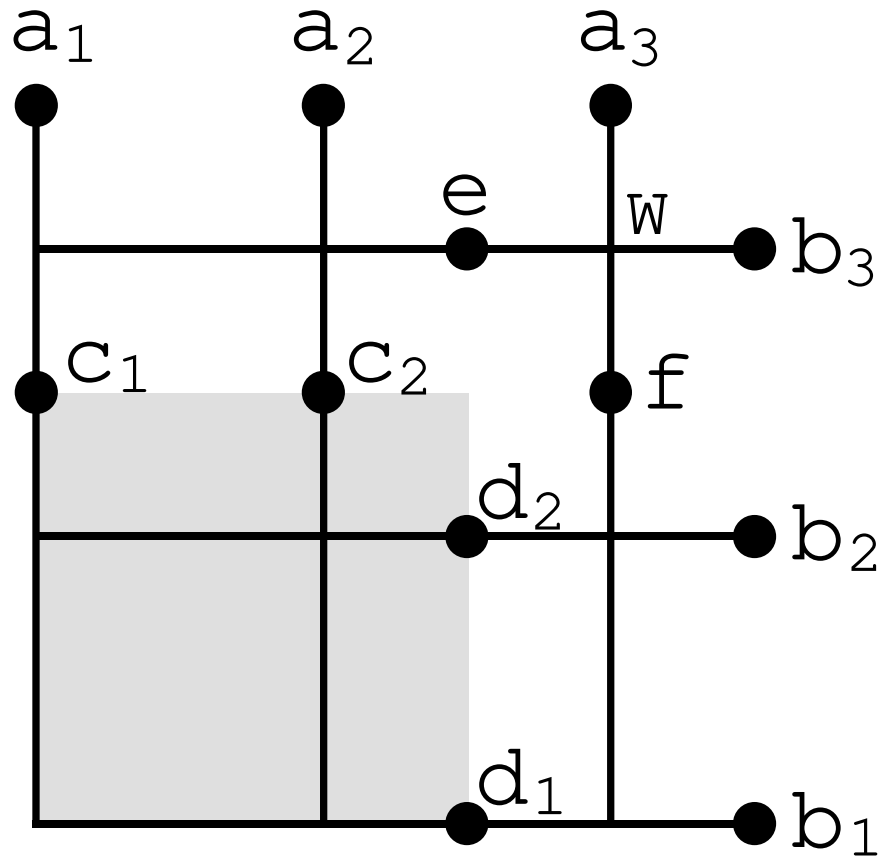
- Fig.2 -

T. Nishino  
K. Okunishi



- Fig.3 -

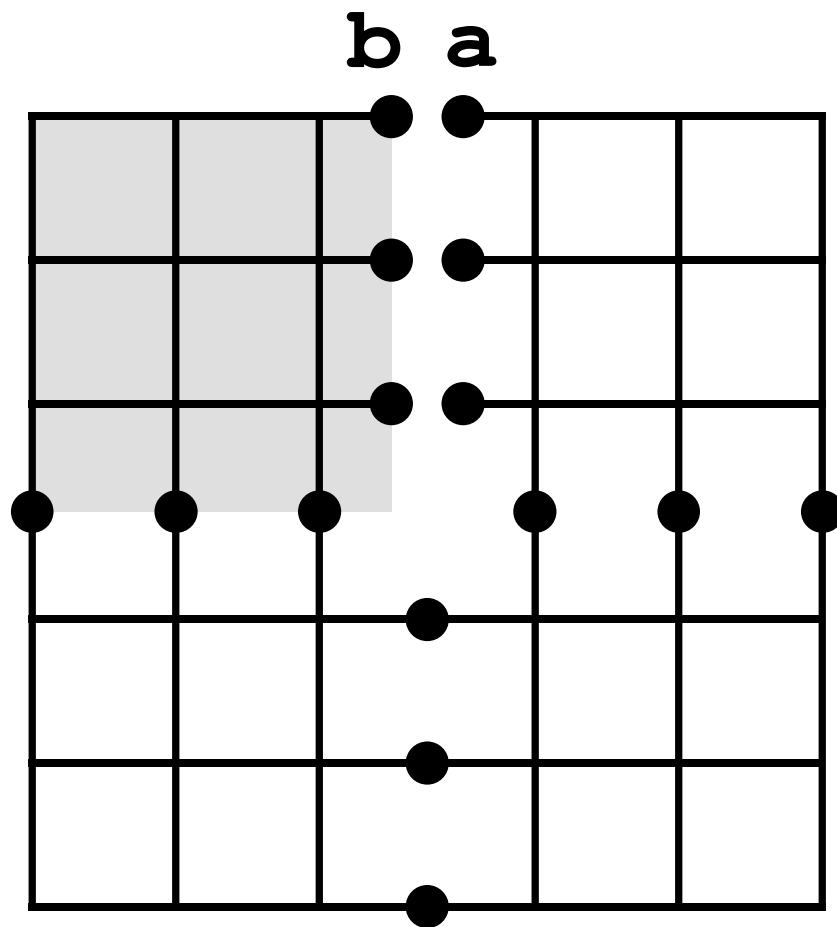
T. Nishino  
K. Okunishi



- Fig.4 -

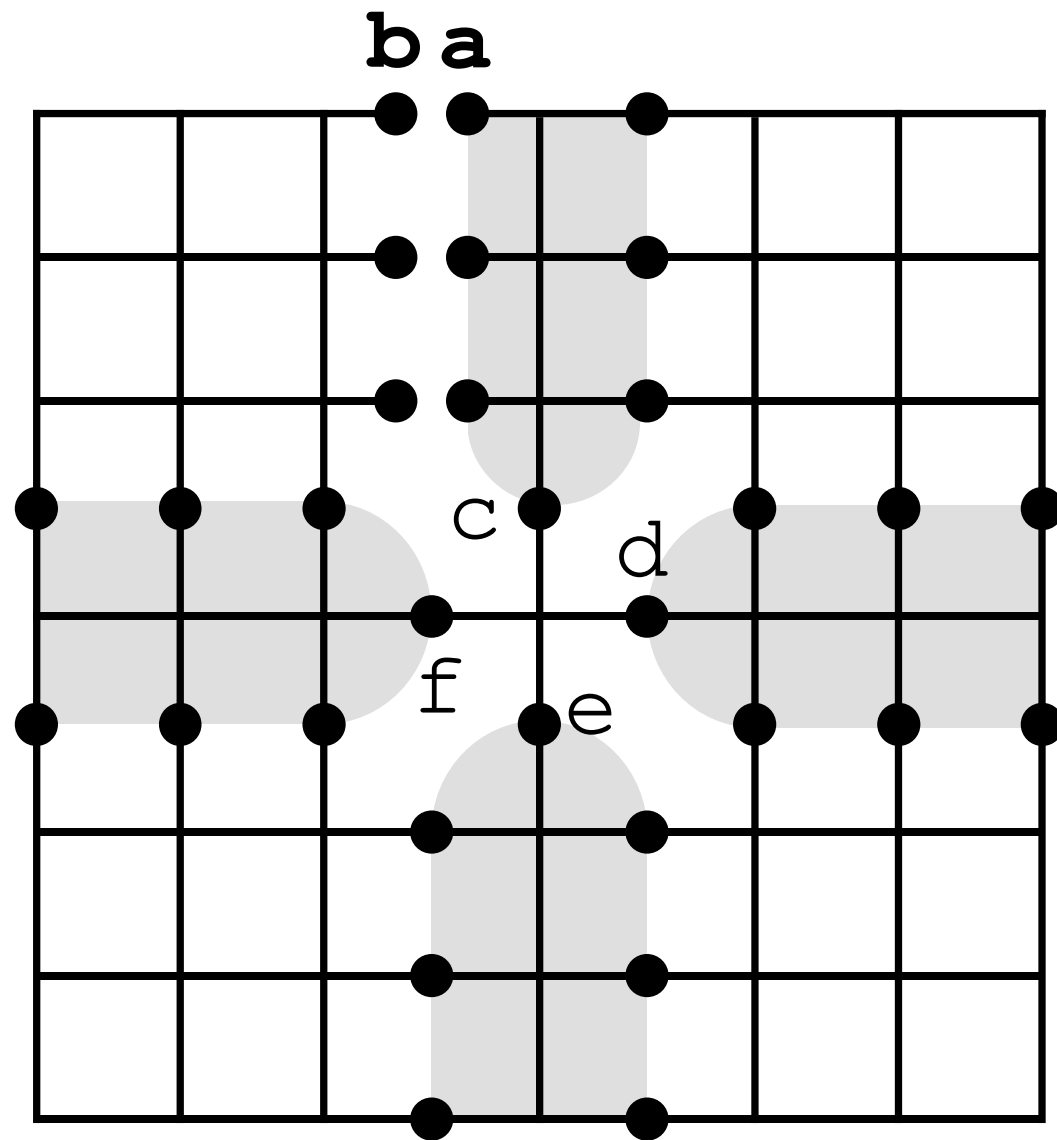
T. Nishino  
K. Okunishi





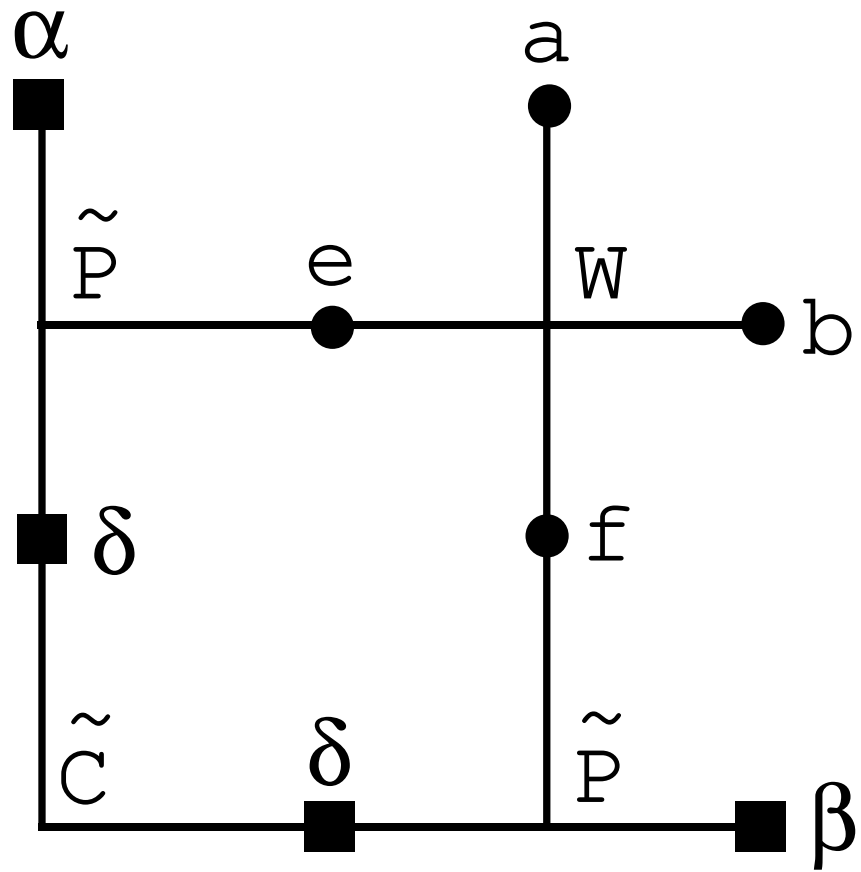
- Fig.5 -

T. Nishino  
K. Okunishi



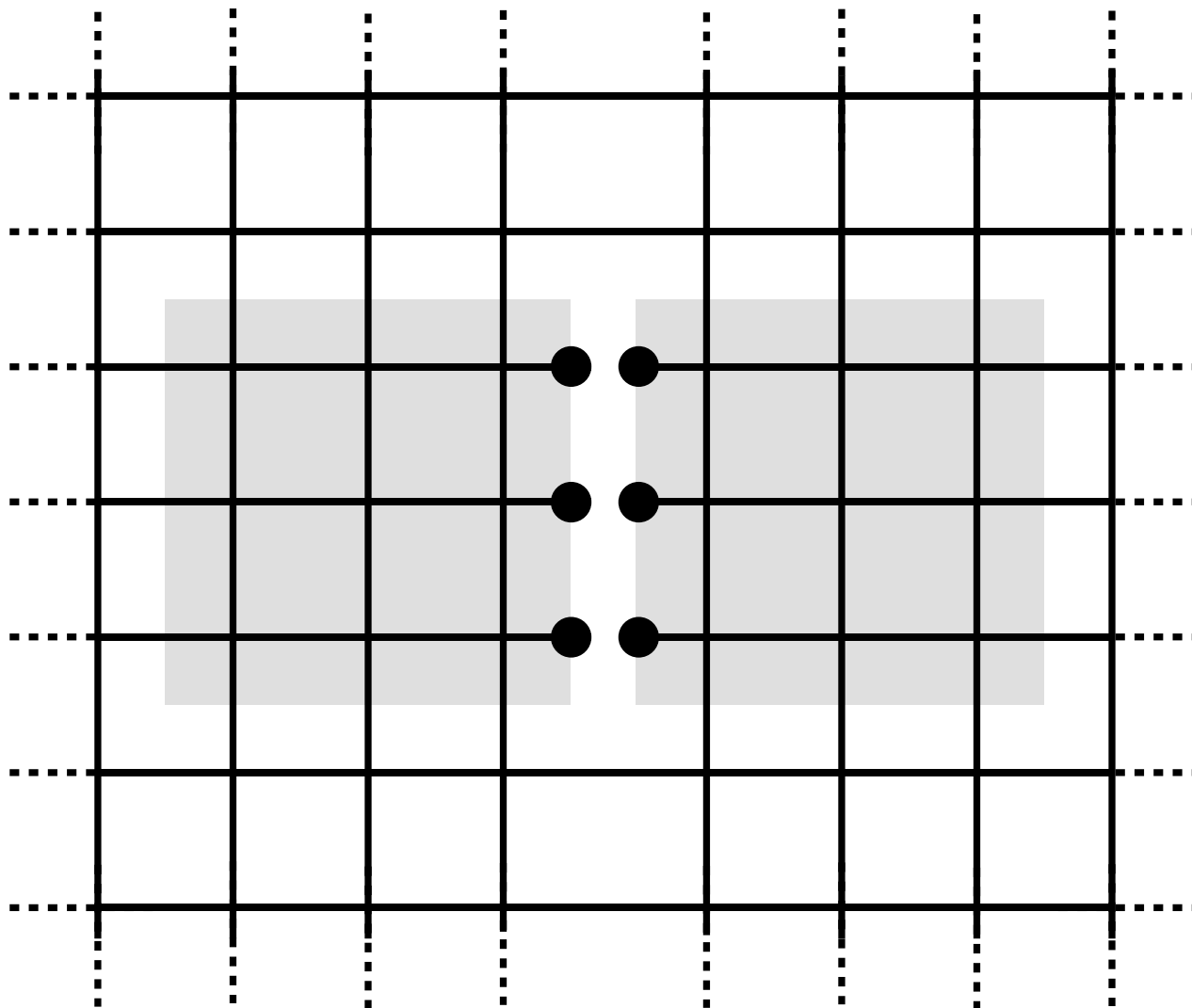
- Fig.6 -

T. Nishino  
K. Okunishi



- Fig.7 -

T. Nishino  
K. Okunishi

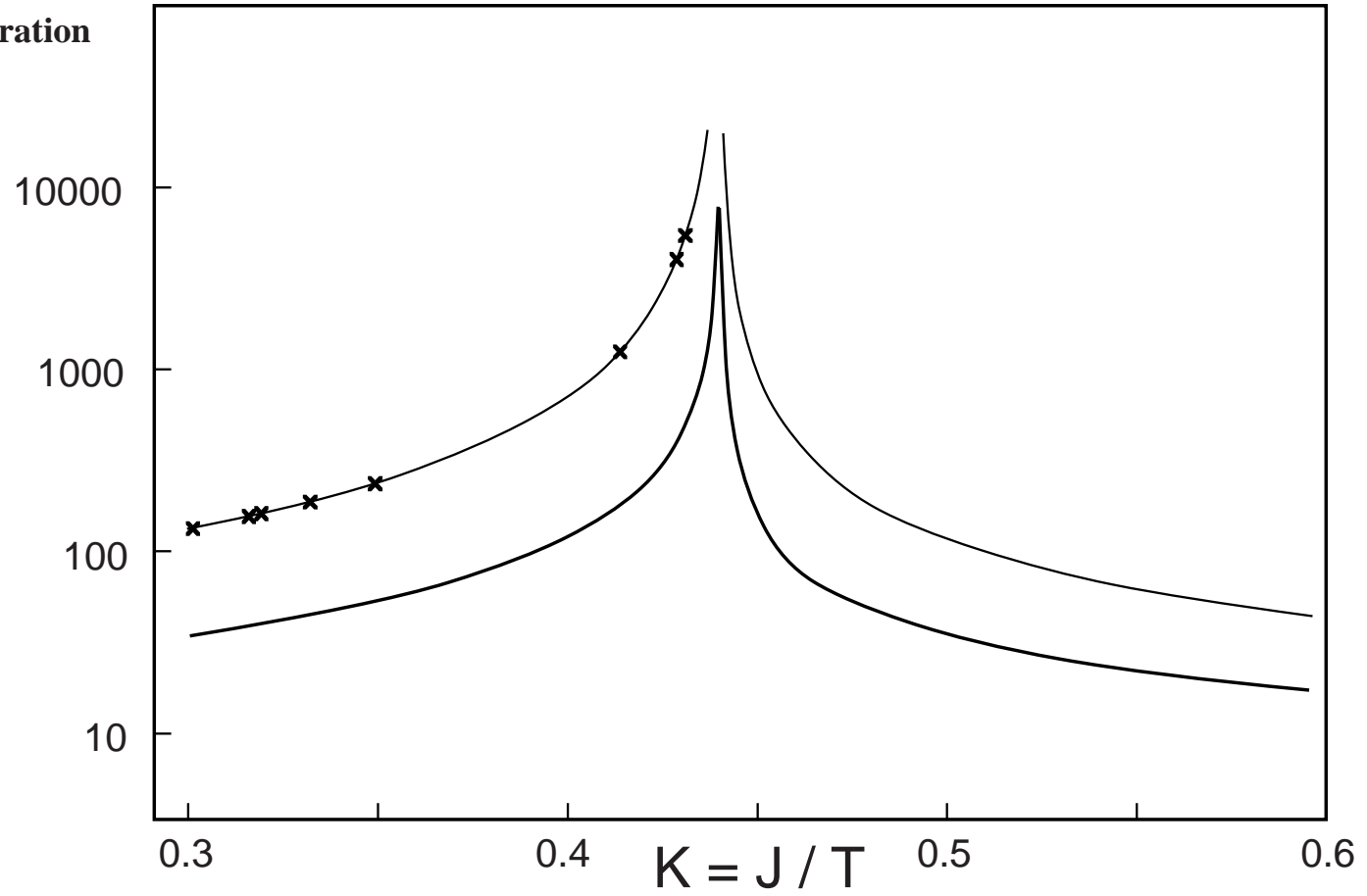


- Fig.8 -

**T. Nishino**  
**K. Okunishi**



**Iteration**



- Fig.10 -

**T. Nishino**  
**K. Okunishi**